creative commons
COMMONS DEED

저작자표시-비영리-변경금지 2.0 대한민국

이용자는 아래의 조건을 따르는 경우에 한하여 자유롭게

- 이 저작물을 복제, 배포, 전송, 전시, 공연 및 방송할 수 있습니다.

다음과 같은 조건을 따라야 합니다:

저작자표시. 귀하는 원저작자를 표시하여야 합니다.

비영리. 귀하는 이 저작물을 영리 목적으로 이용할 수 없습니다.

변경금지. 귀하는 이 저작물을 개작, 변형 또는 가공할 수 없습니다.

- 귀하는, 이 저작물의 재이용이나 배포의 경우, 이 저작물에 적용된 이용허락조건을 명확하게 나타내어야 합니다.
- 저작권자로부터 별도의 허가를 받으면 이러한 조건들은 적용되지 않습니다.

저작권법에 따른 이용자의 권리는 위의 내용에 의하여 영향을 받지 않습니다.

이것은 이용허락규약(Legal Code)을 이해하기 쉽게 요약한 것입니다.

Disclaimer

dCollection

[UCI]I804:48009-200000006410

Doctor of Philosophy

Application of mesenchymal stem cell sheet for prevention of postoperative pancreatic fistula in a rat model

The Graduate School

of the University of Ulsan

Department of Medicine

Seong-Ryong Kim

Application of mesenchymal stem cell sheet for prevention of postoperative pancreatic fistula in a rat model

Supervisor : Song Cheol Kim

A Dissertation

Submitted to
The Graduate School of the University of Ulsan
In partial Fulfillment of the Requirements
For the degree of

Doctor of Philosophy

By

Seong-Ryong Kim

Department of Medicine

Ulsan, Korea

February 2018

Application of mesenchymal stem cell sheet for prevention of postoperative pancreatic fistula in a rat model

This certifies that the dissertation

Of Seong-Ryong Kim is approved

Do Hyun Park

Committee Chair Dr.

Song Cheol Kim

Committee Member Dr.

In Kyong Shim

Committee Member Dr.

Ki Byung Song

Committee Member Dr.

Young-Dong Yu

Committee Member Dr.

Department of Medicine

Ulsan, Korea

February 2018

Abstract

Pancreatic fistula following pancreatic resection (POPF) is a life-threatening complication. Although substantial efforts have been made to minimize the occurrence of POPF, a definitive approach is lacking. We investigated the effect of mesenchymal stem cells (MSCs) sheet for preventing POPF We established a rat model with measurable POPF. Rat adipose derived stem cell (rADSC) and bone marrow derived stem cell (rBMSC) maintained their cell-cell junctions and adhesion proteins with intact fibronectin, as well as characteristics of MSCs. The rats that received rADSC, and rBMSC sheet transplantation showed significantly decreased amount of abdominal fluid compared with the control group, as demonstrated in MR images and the abdominal fluid collected on 1, 3, and 7 days post-operation. Amylase concentration and total amylase contents were significantly lower in the rADSC sheet and rBMSC sheet groups compared with the control groups. rADSC sheet showed increased adhesive and immune cytokine profiles (ICAM-1, L-selectin, TIMP-1), while rBMSC sheets showed reduced immune reaction compared to control and rADSC. Our results show that mesenchymal stem cell sheet technology can be used to prevent POPF, and this new convergent technology has the potential to be translated to clinical settings in order to fulfill the unmet need of POPF.

Contents

Lists of Figures

1. Introduction

Postoperative pancreatic fistula (POPF) is characterized by leakage of digestive enzymes from postoperative and/or damaged pancreas. POPF leads to dissolution of organs and blood vessels, hemorrhage, and sepsis.[1] While mortality rates from pancreatic surgery have been declining due to improvements in surgical intervention and medical technology, pancreatic fistula still occurs at a high rate of 10-40%.[2] There are several techniques for preventing leakage of pancreatic secretion, including handsewn suture, staple,[3] or surgical adhesive materials.[4, 5] Several materials including fibrin glue and polyglycolic acid felt are widely used in clinical settings; however, a definitive approach that prevents pancreatic fistula is still lacking.[6, 7] Materials currently in use are not befitting to prevent pancreatic fistula, as they do not actively induce pancreas regeneration, have limited elasticity, and are difficult to attach to irregularly shaped organs Ideal materials for preventing pancreatic fistula should have the properties of tissue regeneration and wound healing, as well as elasticity and adhesiveness to pancreatic resection margin.

Technologies for utilizing cells to induce wound healing or tissue regeneration are rapidly progressing,[8] especially with mesenchymal stem cells (MSCs) that have functions in both regeneration and immune response. Recently, some clinical applications of MSCs have been reported. While traditional cell therapies often rely on direct single cell injection, application onto topical regions is impractical due to massive cell loss and the low survival rates of single cells. Hence, new techniques for efficient cell transplantation are needed. In this regard, scaffold-free cell sheets are one of the prevalent cell therapy methods used clinically. Conventional cell therapy methods harvest cells by using chemical treatment such as trypsin-EDTA and dispase, or physical force, which leads to cells losing their inherent properties. Cell sheets, on the other hand, are harvested by controlling the culture temperature, thus enabling them to maintain cell-cell connections and adherence protein layers that facilitate

attachment to tissue surface.[9, 10] Successful regeneration of cornea and esophagus with cell sheet technology in clinical trials have been previously reported.[11-13] We hypothesized that MSC sheet would be able to attach onto the pancreas resection site to induce tissue regeneration, wound healing, and immune modulation of pancreas resection site.

Although pancreatic fistula is a clinically significant complication following pancreatic surgery, a valid animal model that enables assessment of materials that may prevent pancreatic fistula has not yet been established. Previous pancreatic fistula animal models that utilized rats, dogs, or pigs were usually studied with short and limited observation periods, and thus were not able to comprehensively represent the clinical situation. In this study, we developed a rat model of POPF and examined its survival rate and abdominal fluid volume across an extended period to establish an appropriate disease model that recapitulates clinical situations. Using this rat model of POPF and MSC cell sheets, we evaluated the ability of MSC cell sheets for preventing POPF.

2. Materials and Methods

2.1. Fabrication of mesenchymal stem cell sheet

Adipose tissue and bone marrow stem cells were extracted and isolated from seven-week SD-wild type rat, SD-TG (CAG-EGFP) (JapanSLC, Hamamatsu, Japan). Adipose tissue was harvested from the inguinal region and minced into small cubic-shaped fragments. 1 mg/ml of Collagenase type I (Worthington Biochemical Corporation, NJ, USA) was used to digest the adipose tissue. rADSC were isolated from minced adipose tissue by gravity, and rBMSC were isolated from collecting attached cells after flushing the marrows of femur and tibia. To isolate rBMSC, a syringe was inserted into one open end of each of the greater trochanter, epicondyle, tibia head, and medial malleolus of the femur to flush the marrow out into a 100

mm dish. The extracted bone marrow was incubated for 12 hours, followed by a medium change every day for five days. rBMSC were obtained through subsequent subcultures. rADSC and rBMSC were cultured in Dulbecco's Modification of Eagle's Medium (DMEM; GIBCO, Carlsbad, CA, USA) mixed with 10% fetal bovine serum (FBS; GIBCO, MD, USA) and 1% anti-antibiotics (AA; GIBCO, MD, USA) in a 37 °C, 5% CO_2 chamber.

The isolated rADSC and rBMSC were cultured on temperature-responsive dishes (3.5 mm UpCell™: Thermo Fisher Scientific, MA, USA) to fabricate rADSC and rBMSC sheets, respectively. Cell sheets were fabricated from passage 3 cells. $1.1x10^6$ ADSCs and BMSCs were seeded and cultured for two-three days. The cells were transported to a lower temperature chamber at 20 °C an hour before the transplantation operation and were prepared into a cell sheet form. Figure 1A shows the scheme of rADSC and rBMSC isolation and fabrication of cell sheet (rADSCs sheet: left panel and rBMSCs sheet: right panel). The UpCell dishes are hydrophobic at 37 °C but become hydrophilic at 20 °C and allows the cell sheets to detach from the dishes while maintaining their cell-cell junctions and adhesion molecules (Fig. 1B). The cell sheets were attached to CellShifter™ membranes (Thermo Fisher Scientific, MA, USA) that were then transplanted onto the pancreas resection area (Fig. 1C).

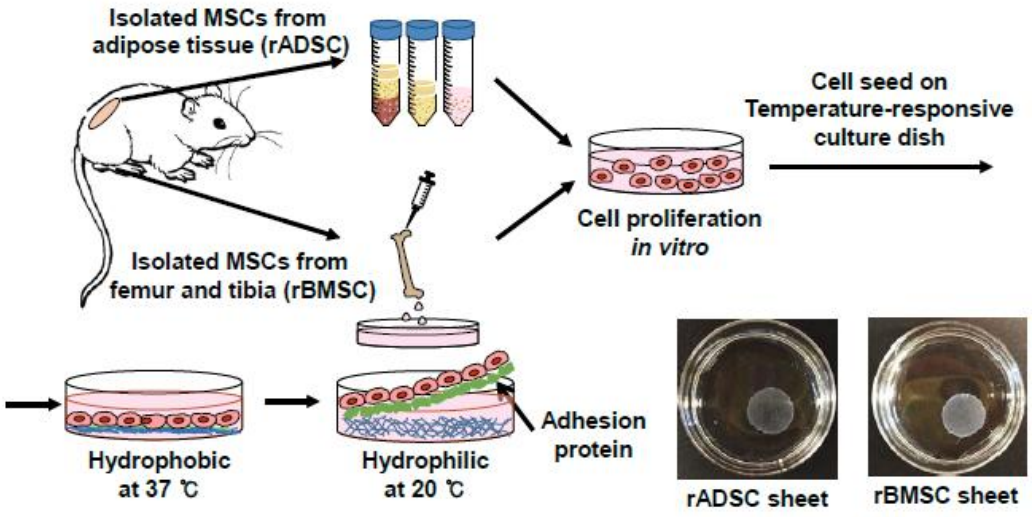

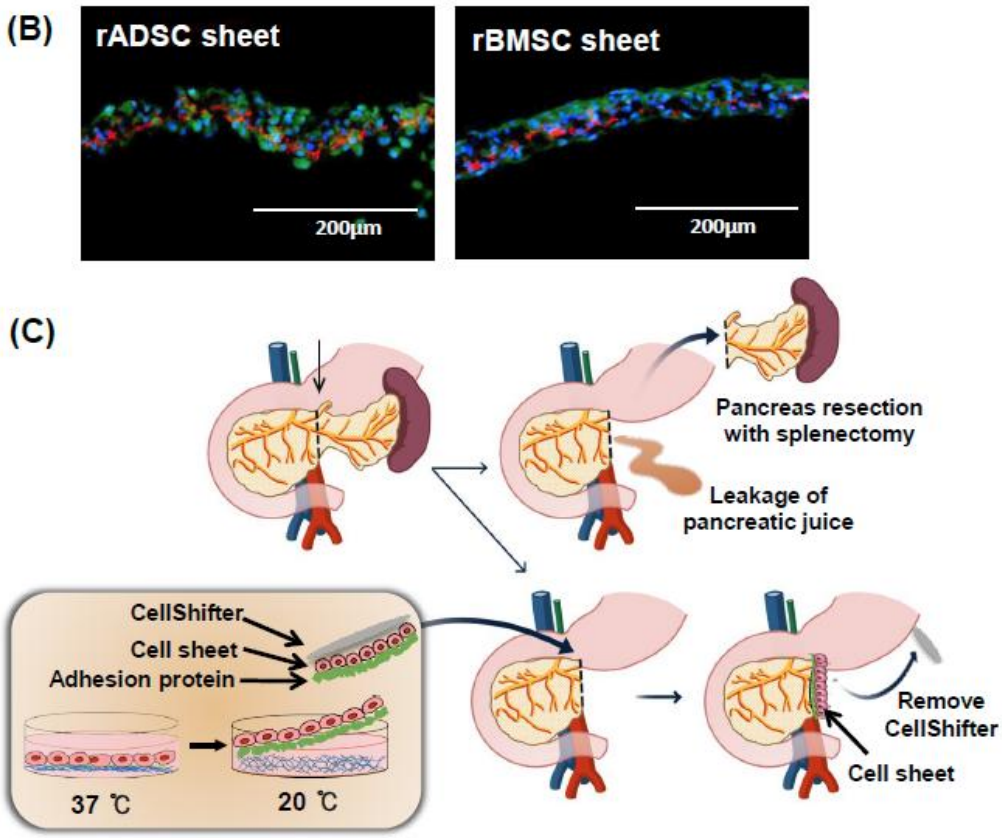

Fig. 1. Study design of mesenchymal stem cell sheet for preventing postoperative pancreatic fistula. Schematic diagram of rADSC and rBMSC isolation from rats, and rADSC and rBMSC sheet fabrication using temperature-responsive culture dishes. rADSC and rBMSC were cultured for two days and were allowed to reach confluence. At this point, the culture temperature was lowered from 37 ℃ to 20 ℃ in order to harvest the cell sheet. (B) Extracellular matrix accumulation of rADSC and rBMSC sheet. Fibronectin was detected with immunofluorescence. Scale bars represent 200 μm. Green: rADSC or rBMSC from GFP transgenic rat, Blue: nucleus, Red: fibronectin (C) Schematic description of the experimental procedure of pancreas resection model and application of cell sheet.

2.2. Establishment of rat model of postoperative pancreatic fistula (POPF)

SD-Rats (ORIENT BIO, Seongnam, South Korea) between 8-12 weeks old were used in the experiments. They were bred in a room maintained at 22-24 °Cand a 12-hour light-dark cycle. Animal experiments were performed in accordance with the guidelines of Institutional Animal Care and Use Committee of Asan Institute for Life Sciences. Three different rat models of POPF were developed—1) model I (common pancreatic duct division model): division of the pancreas where the common duct of pancreas and bile duct intersect, 2) model II (gastric and splenic duct division with distal pancreatectomy and splenectomy

model): division of both gastric duct and splenic duct at the left margin of the portal vein, and 3) model III (splenic duct division with distal pancreatectomy and splenectomy model): Removal of splenic duct at the pancreas tail level from spleen. The survival rates and abdominal fluid volumes of these three models were compared for 10 days after pancreas resection. The experimental procedure is as follows: Rats were anesthetized with zoletil (50 mg/kg) and Rompun (10 mg/kg) and were laid down in the supine position. A midline incision was performed on the abdomen. By holding the stomach with an atraumatic forceps, the duodenum and spleen were pulled out. Through omentectomy, the stomach and spleen were mobilized and the short gastric vessel was separated after ligating with a black silk 4-0 tie. The portal vein was recognized once the area between the colon and pancreas was mobilized. After determining the resection surface of the pancreas left to the portal vein, the resection surface was fixated with a forcep, and the pancreas parenchym was crushed with another forcep. Shear stress was applied in a direction parallel to the vessel, which left the vessel intact but tore the duct. The vessels were then tied with black silk 7-0 and resected. Ducts were left divided. The survival rate for 10 days from all three models and the amount of postoperative fluid were measured (n=10).

2.3. Characterization of mesenchymal stem cells

To determine the mesenchymal stem cell (MSC) characteristics of the isolated rADSCs and rBMSCs, we examined the expression of MSC surface markers. rADSC and rBMSC at passage 3 was harvested with trypsin. After being blocked with 2% BSA, a total of 1 x 10^5 cells were resuspended in 200 μl PBS for each reaction. Cells were incubated on ice for 1 hr at 4 °C with the following anti-human antibodies; PE-anti-rat CD29, PE-anti-rat CD 31, PE anti-rat CD45 (BD PHARMINGEN, NJ, USA), IgG FITC-isotype control, FITC-anti-rat MHC CLASS I, FITC-anti-rat CD90 (Abcam, Cambridge, UK) by 1:1000. The antibodies were incubated at 4 °C for 30 minutes and washed with PBS. Cells were analyzed by flow

cytometry (FACS Caliber, Canto: BD Bioscience, San Jose, CA, USA).

To induce osteogenic and adipogenic differentiation, cells at passage 3 were plated on 6-well plate at 4,000 cells/cm^2 with complete culture media and were cultured until confluency. At this point, the culture media was replaced with either the adipogenic or osteogenic differentiation media (hMSC Osteogenic Differentiation BulletKit Medium, PT-3002 and hMSC Adipogenic Differentiation BulletKIt Medium, PT-3004; Lonza Japan, Tokyo) and was changed every three days. After 14 days in culture, the adipogenic culture formed adipose-like vacuoles. The plates were fixed with 4% paraformaldehyde for 20 minutes and stained with Oil Red O (Sigma-Aldrich, St Louis, MO, USA). The osteogenic differentiation cultures were incubated for 28 days; the cells were then fixed and stained with 1% Alizarin Red solution pH 4.1 (Sigma-Aldrich, St Louis, MO, USA), which allowed for calcium deposits to be stained orange-red. The green fluorescence of cells from SD-TG (CAG-EGFP) and fibronectin of the sheet was confirmed by fluorescence microscopy (EVOS^{TM} FL Auto Imaging System, ThermoFisher Scientific, Massachusetts, USA). To stain fibronectin of the cell sheet, the cell sheet was embedded in paraffin and sliced into 4 um-thick cross-sections. The slices were stained with primary fibronectin antibody (sc-8422; Santa Cruse Biotechnology, Inc., CA, USA) and secondary anti-mouse Goat Anti-Mouse Alexa Fluor® 555(Abcam, Invitrogen, Thermo Fisher Scientific, MA, USA) at 1:100 dilution.

2.4. Optical imaging of the GFP rADSC and rBMSC sheet

To observe the attached rADSC and rBMSC sheet on the pancreatic resection site, green fluorescence of rADSC and rBMSC from GFP rats were detected by IVIS Spectrum system (Caliper Inc., Alameda, CA). For organ (*ex vivo*) imaging, fresh organs were placed on plates and analyzed. EGFP was excited at 488 nm (filter range 445 to 490 nm) and detected at 510 nm. The region of the interested (ROI) level was measured with radiance (photons/s/cm^2/sr) using an analysis program, Living Image 4.4 (Caliper Life Sciences, PerkinElmer Inc.).

2.5. Magnetic resonance (MR) imaging

9.4 T/160 mm scanner (Agilent Technologies, Palo Alto, CA, USA) with 400 mT/m gradient sets was used for MR imaging of fluid collection in the abdomen. All rats were anesthetized in a 1.5 - 3.0% concentrated isoflurane inhalation chamber with a 5:5 mixture of N_2O and O_2 gas. Transverse images from the top of the liver to the bottom of the bladder were sliced into 30 pages of 1.5 mm thickness (matrix = 192 × 256; field of view = 3.0 × 4.0 cm; section thickness = 1.5 mm; section gap = 0.33 mm; and a number of sections = 30 sections with the longitudinal axis on the bottom). Longitudinal images from the top of the abdomen to the bottom were sliced into 20 pages of 3.0 mm thickness. (Sequence parameters: matrix size = 192 × 256; field of view = 4.5 × 5.5 cm; section thickness = 3.0 mm; section gap = 0.5 mm). Location of the organs and fat was obtained in the T1 image, and images of water were obtained in T2. T2 images were analyzed with the program image J (DICOM image by National Institutes of Health, MD, USA).[14, 15]

2.6. Amylase assay in abdominal fluid

Following euthanasia, rat abdominal fluid was collected via a 10ml syringe and transferred into a tube. The fluid was frozen at -80C after its volume was recorded. Amylase concentration was measured with amylase activity kit (Abcam, Cambridge, UK). The frozen fluid collection was slowly thawed in ice. Fluid collection diluted in autoclaved distilled water (1:1000) was used to establish experimental conditions within the standard range. The assay procedures were followed from the manufacturer's instructions. Amylase level was calculated by multiplying the amylase concentration and the abdominal fluid volume.

2.7. Immune cytokine analysis

Rat immune cytokine array kit (R&D SYSTEMS, MN, USA; #ARY008) was used to carry out immune cytokine analysis. The tissue section 3 mm towards the pancreas head from the pancreas resection surface was used. The tissue was soaked in PBS with protease inhibitor

(SIGMA-Aldrich) and homogenized. 1% Triton x-100 of the final concentration was added and mixed well, followed by freezing. The mixture was then thawed and centrifuged. The resulting supernatant was used for analysis. 400 μ g of protein was used per membrane based on protein quantification. The subsequent steps were directed by the manufacturer's instructions. The experimental groups included normal rats that did not undergo any operation, DP that only underwent pancreatic resection operation, and two experimental groups in which rADSCs sheets and rBMSCs sheets were attached to the resection surface, respectively. Interleukins, activators of B lymphocytes, activations of natural killers, and multiple biological effectors were identified with this kit.

2.8. Immunohistochemistry and H&E staining

The rats were sacrificed either on day 1 or 3, and their pancreas was removed and fixed with 4% formalin. A paraffin block was prepared with the fixated tissue, and the block was cut into 4 μm sections. To perform hematoxylin and eosin (H&E) staining, samples were deparaffinized and dehydrated, followed by applying hematoxylin (Sigma-Aldrich, MO, USA) and eosin staining (Sigma-Aldrich, MO, USA). Mounting was performed with Histomount (Thermo Fisher Scientific, MA, USA). The tissue slides were deparaffinized and dehydrated using xylene, and 100%, 95%, 70% ethanol. A vegetable steamer and citrate buffer were used to retrieve antigens from the samples. Samples that underwent antigen-retrieval were blocked with 1% BSA. Immunohistochemistry was performed using primary antibodies for GFP (dilution 1:1000, Abcam, Cambridge, UK). Formalin-fixed, paraffin-embedded sections (4 μm in thickness) were deparaffinized, dehydrated through a graded alcohol series, blocked with hydrogen peroxide, and dried for 10 minutes at RT then for 20 minutes in an incubator at 65 °C. An automated slide preparation system (Benchmark XT; Ventana Medical Systems Inc., Tucson, AZ, USA) with OptiView DAB Detection Kit (Ventana Medical Systems) was used for immunohistochemistry.

2.9. Statistical analysis

Statistical significance was determined using GraphPad Prism 5 (GraphPad Software, San Diego, CA, USA). Statistical significance of the differences between groups was analyzed with Student's t-test and a two-way analysis of variance. $P < 0.05$ was used as the cut-off for determining statistical significance. The data are presented as the mean ± standard deviation, with the number of samples indicated in the figure legends.

3. Results

3.1. Fabrication and characterization of mesenchymal stem cell sheets

To confirm whether the cultured rADSCs and rBMSCs carry the properties of mesenchymal stem cells, flow cytometry was performed with surface marker antibodies. The results were positive for CD29 and CD90, and negative for CD31, CD45, MHC class 1 (Fig. 2A). Mesenchymal cells are also able to differentiate depending on the surrounding environment including adipogenesis and osteogenesis (Fig. 2B). Adipogenesis and osteogenesis were verified with oil red O staining and alizarin red staining, respectively. The lipid drops from the mesenchymal stem cells were stained red through the oil red O staining method, and calcium deposits were stained red through the alizarin red staining method, and successful adipogenesis and osteogenesis of the separated mesenchymal stem cells were confirmed. These results show that cells separated from rats retain the properties of mesenchymal stem cells and that they are successful in fabricating cell sheets. Also, to track the transplanted cells into the transplanted site, we isolated rADSCs and rBMSCs from GFP transgenic rats (Tg-CAG-GFP). Strong green fluorescence was observed in the cells and sheets made of rADSCs and rBMSCs.

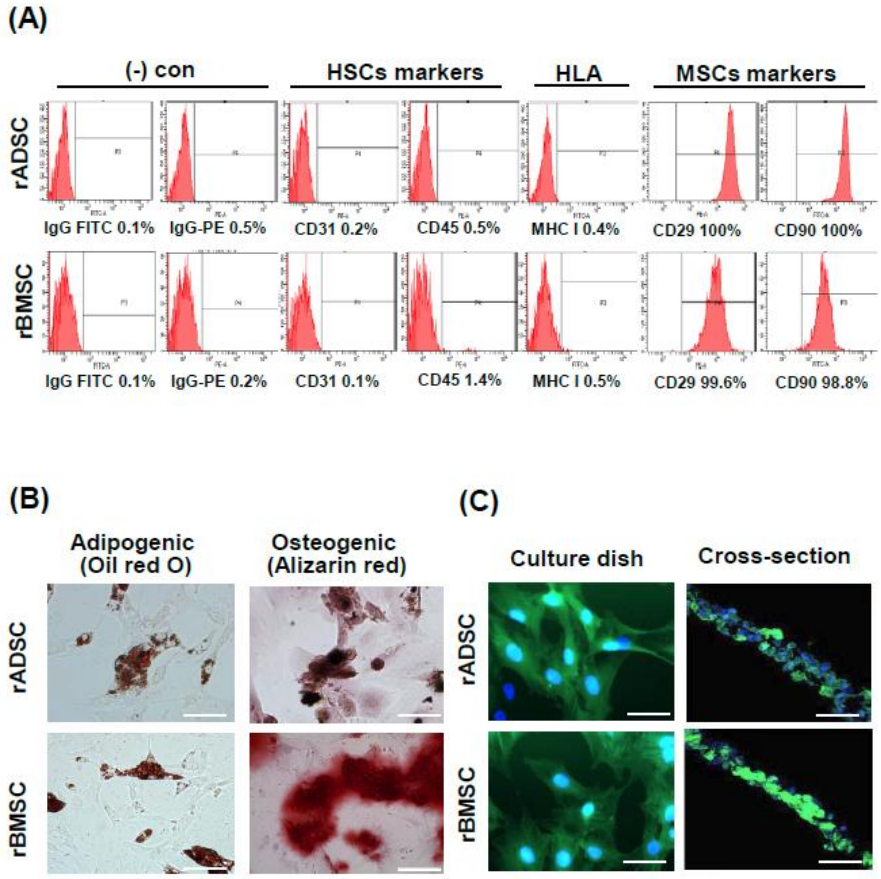

Fig. 2. Confirmation of the characteristics and biopotency of rADSCs and rBMSCs obtained from a GFP transgenic rat. (A) The expression of surface antigens on rADSC and rBMSC analyzed by flow cytometry. (B) Oil Red O and alizarin red staining of rADSC and rBMSC. Scale bars represent 200 μm. (C) Fluorescence images of mesenchymal stem cells from GFP transgenic rats and the cross-section of a cell sheet. Green: rADSC or rBMSC from GFP transgenic rat, Blue: nucleus.

3.2. Establishing rat model of postoperative pancreatic fistula (POPF)

Figures 3A and 3B shows the resection site in the images of rat pancreas. Three different modeling procedures were developed including model I (common pancreatic duct division), model II (gastric and splenic duct division with distal pancreatectomy and splenectomy), and model III (splenic duct division with distal pancreatectomy and splenectomy); each model's survival rate and abdominal fluid volume at 10 days after pancreas resection were analyzed. Survival rate and abdominal fluid volume of each model are shown in Figures 3C and 3D, respectively. In model I, 5.77 ± 1.29 of fluid was observed due to pancreatic fistula, but all

rats died on day 1 (n = 10). Model III rats survived for the whole experimental period (10 days), but no fluid was observed during after surgery. Model II survived for the whole experimental period, with continuous secretion of pancreatic juice, and 4.85±0.31 ml of fluid was observed on day 1 (n = 10). Thus, model II—hereafter referred to as distal pancreatectomy (DP)—was deemed as the adequate model for assessing the efficacy of materials for preventing POPF.

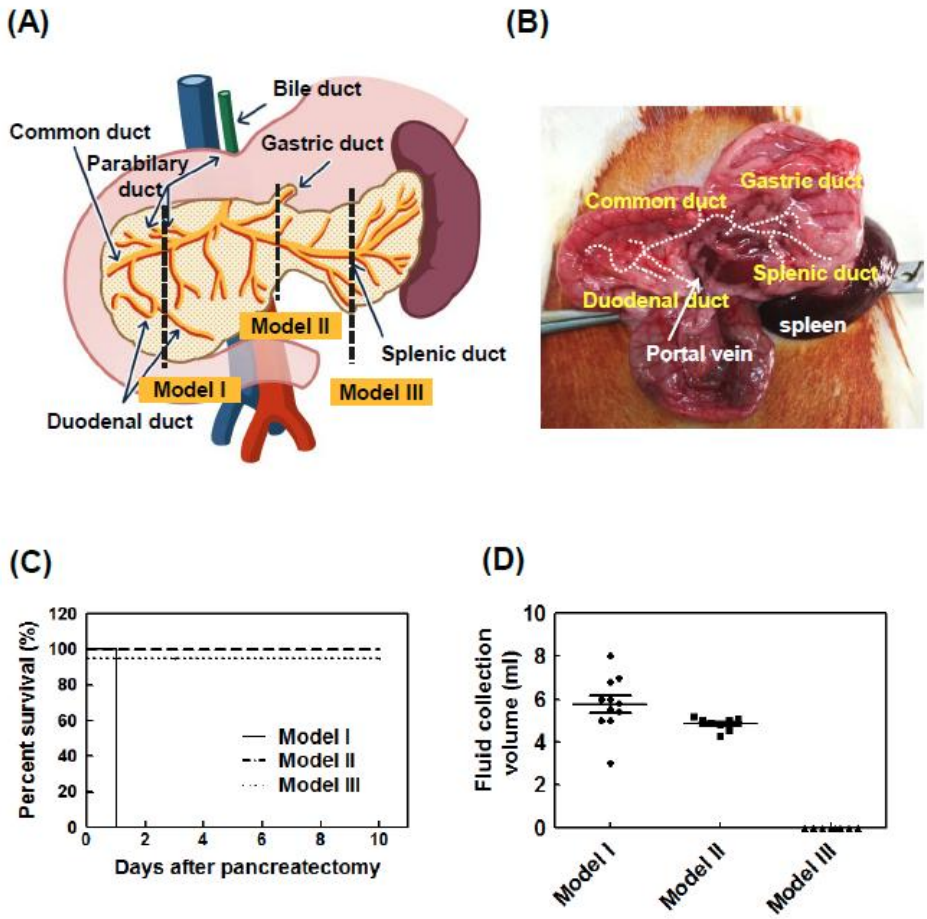

Fig. 3. Establishment of a rat model of postoperative pancreatic fistula (POPF). (A) Schematic representation of rat pancreas and the resection sites of models I, II, and III. Model I (common pancreatic duct division model): division of the pancreas where the common duct of pancreas and bile duct intersect, Model II (gastric and splenic duct division with distal pancreatectomy and splenectomy model): division of both gastric duct and splenic duct at the left margin of the portal vein, and Model III (splenic duct division with distal pancreatectomy and splenectomy model): Removal of splenic duct at the pancreas tail level from spleen. (B) Photos of rat pancreas, pancreatic duct, and portal vein. (C) The survival rates of models I, II, and III (n = 10 each). While all model I rats died on day 1 after pancreatectomy, all model II and III rats survived during the experimental period. (D) The abdominal fluid volume of each model on day 1 after pancreatectomy (n = 10 each).

3.3. Attachment of cell sheet on pancreas resection surface

Figure 4A shows the process of attaching cell sheets to the pancreas resection site. As shown in Figure 4A (upper left), the pancreatic juice was secreted only where the duct was opened, which is the optimal location for attaching the cell sheet. After pancreas resection, cell sheet was attached using CellShifter^{TM} on the resection surface. After five minutes, which is a sufficient time for the cell sheet to attach to the resection site, the shifter was removed, leaving behind only the cell sheet. Figure 3B shows the representative IVIS image of GFP signals on the cell sheets. To confirm the attachment of rADSC and rBMSC sheet on the pancreatic resection site, green fluorescences of rADSC and rBMSC from GFP rats were detected by IVIS Spectrum system an hour later and one day after cell sheet transplantation. To avoid autofluorescence from rat hair, fresh organs including liver, stomach, remaining pancreas, and intestine were harvested, imaged, and analyzed. Strong green fluorescence of GFP cells was detected on the pancreas resection site at an hour and one day post-operation. No significant difference was observed between rADSC sheet and rBMSC sheet in terms of GFP fluorescence.

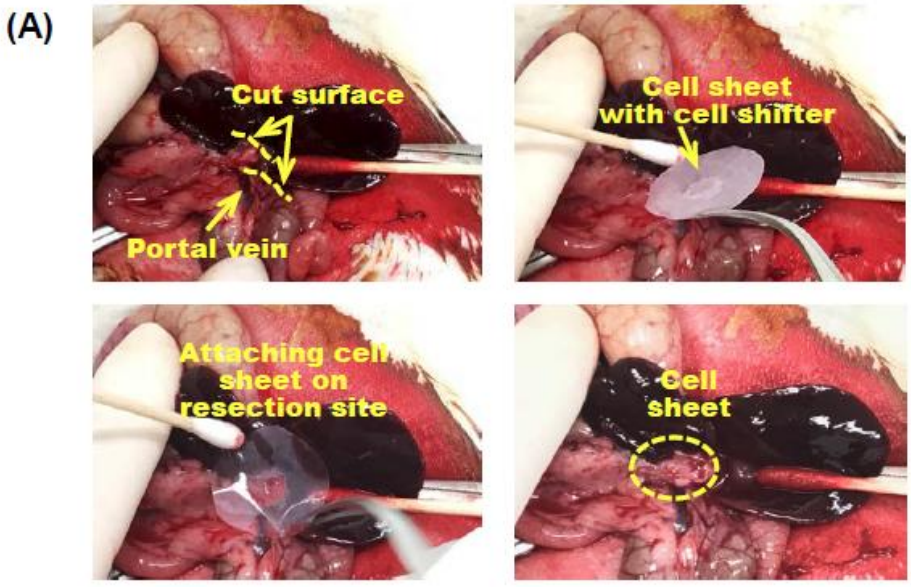

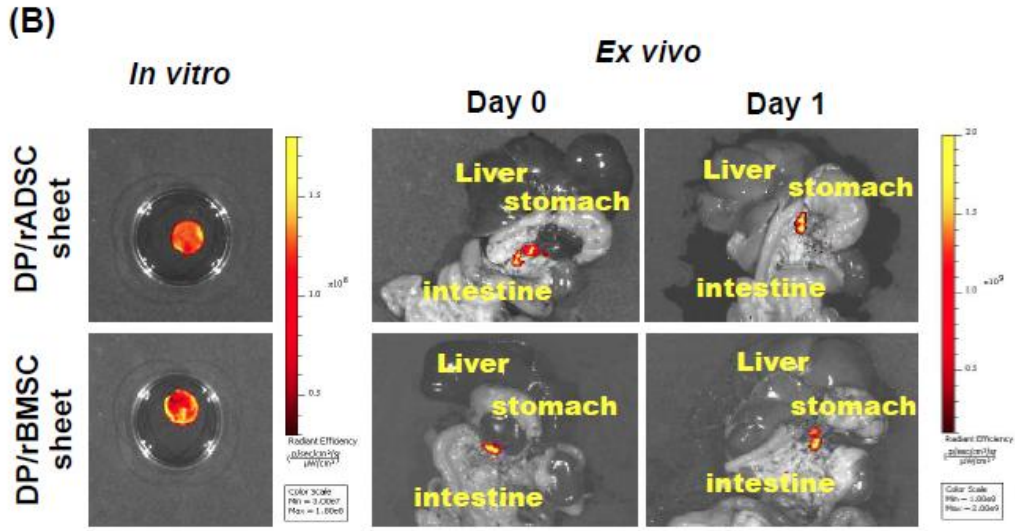

Fig. 4. Attachment of cell sheets onto the pancreas resection surface. (A) Photos of the pancreas resection procedure and application of cell sheet onto the resection site. Pancreatic juice was secreted only where the duct was opened (upper left). Preparation of cell sheets using CellShifterTM (upper right). Following pancreas resection, cell sheet was attached on the pancreatic resection surface (lower left). After five minutes, the shifter was removed, and only the cell sheet remained (lower right). (B) Representative IVIS image of GFP signal of a cell sheet in vitro and ex vivo. rADSC and rBMSC sheet showed strong green signals in vitro. Green fluorescence of rADSC and rBMSC sheet were observed in ex vivo image an hour later and a day after cell sheet transplantation.

3.4. Efficacy of cell sheets in preventing POPF

DP model without cell sheet attachment (control), DP with rADSCs sheet attachment, and DP with rBMSCs sheet attachment were compared experimentally. To confirm the efficacy of cell sheets in preventing pancreatic juice leakage, abdominal fluid volume was collected and measured on days 1, 3 and 7. As shown in Figure 5A, abdominal fluid retrieved from the control group was 4.99 ± 0.63 ml on day 1, 4.58 ± 1.39 ml on day 3, and 2.93 ± 1.76 ml on day 7 (n=9); abdominal fluiud retrieved from the rADSCs sheet attachment group was 1.50 ± 1.43 ml on day 1, 0.71 ± 0.16 ml on day 3, 0.31 ± 0.31 ml on day 7 (n=9), and that retrieved from the rBMSC sheet attachment group was 0.55 ± 0.80 ml on day 1, 0.50 ± 0.10 ml on day 3, and 0.10 ± 0.00 ml on day 7 (n = 9). There was a significant reduction in fluid collection from both rADSC and rBMSC cell sheet attachment groups as opposed to the

control group (Control vs rADSCs; $p < 0.001$ on day 1 and day 3, $p = 0.005$ on day 7, Control vs rBMSCs; $p<0.001$ on day 1 and day 3, $p = 0.002$ on day 7). There was no significant difference between rADSC and rBMSC sheet groups on day 1 and 7 ($p = 0.101$ at day1and $p = 0.108$ at day7). However, rBMSCs showed smaller ascites volume than rADSC on day 3 ($p = 0.004$).

MR imaging showed a similar tendency in terms of ascites volume level. MR scans were taken on day 1, 3, 7 for the control group and the cell sheet attachment group. The area of the fluid collection was shown in ImageT2 which appeared bright (Fig. 5B). For the longitudinal section, the area of the fluid collection was measured on the kidney image. For transverse image, the liver was sectioned from the top at 3 mm intervals and a total of thirty images were obtained. The control POPF rat showed abdominal fluid on day 1, 3 and 7 days after surgery, as shown in the white area. The rat with rADSC and rBMSC sheet attachment showed considerably less abdominal fluid after surgery.

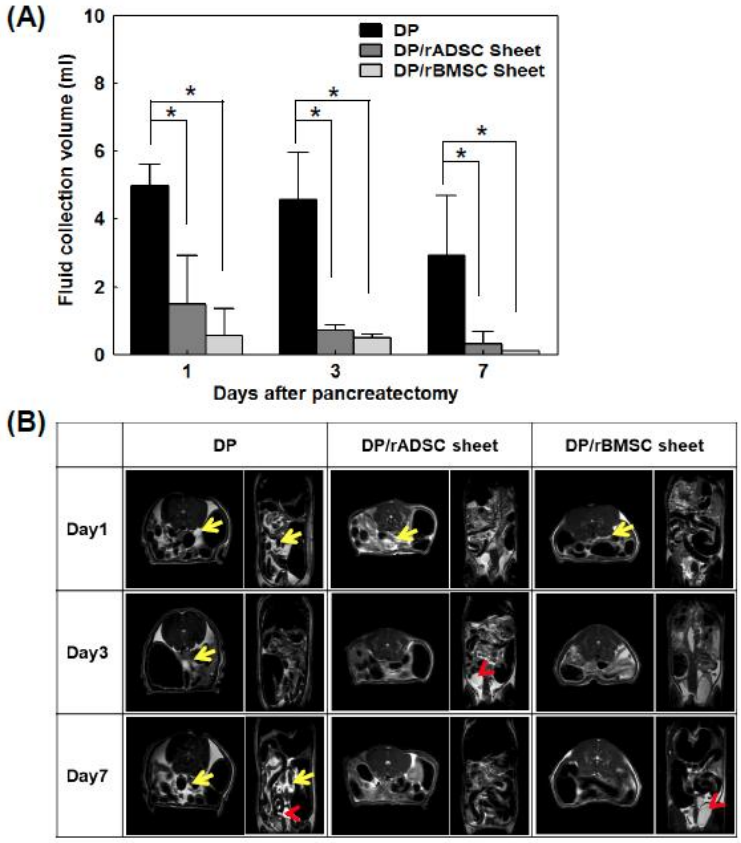

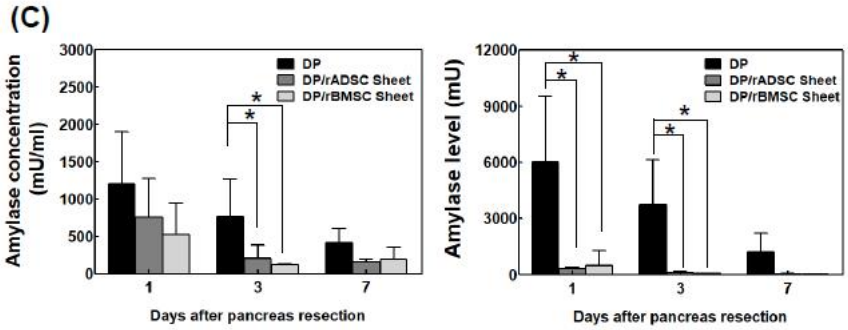

Fig. 5. Confirming efficacy of cell sheets in preventing POPF. Control group (DP model without cell sheet attachment), DP with rADSCs sheet attachment, and DP with rBMSCs sheet attachment were compared experimentally. (A) Abdominal fluid was retrieved from each group on days 1, 3 and 7 after pancreatectomy. * $p < 0.05$. (B) Representative MR imaging of each group. The right panel of each image is the transverse section and the left panel is the longitudinal section. Yellow arrow indicates the abdominal fluid (white area). Yellow arrow ahead indicates water in the kidney. (C) Amylase concentration was analyzed on days 1, 3, and 7 to confirm the presence of pancreatic juice in abdominal fluid. Amylase concentration decreased over time in all groups. Amylase concentration tended to increase in the control group compared to that of the rADSC sheet and rBMSCs sheet group. Total amylase level was calculated by multiplying the amylase concentration and the abdominal fluid volume.

3.5. Measurement of amylase level from abdominal fluid collection

To confirm the presence of pancreatic juice in the abdominal fluid collection, amylase concentration and level were measured (Fig. 5C). Amylase concentration decreased over time in all groups. Amylase concentration tended to increase in the control group compared to the rADSC sheet and rBMSCs sheet groups. Specifically, amylase concentration of the control group was significantly higher than that of the sheet group on day 3 ($p = 0.015$ in rADSCs sheet and $p = 0.042$ in rBMSCs sheet). Amylase concentration was measured as 1209.58 ± 691.69 mU/ml, 758.84 ± 505.87 mU/ml, 408.08 ± 196.78 mU/ml in the control group, 753.14 ± 515.00 mU/ml, 208.24 ± 171.34 mU/ml, 155.98 ± 34.98 mU/ml in the rADSC sheet attachment group, and 530.35 ± 414.61 mU/ml, 119.70 ± 10.88 mU/ml, 199.14 ± 154.57 mU/ml in the rBMSC sheet attachment group on day 1, 3 and 7, respectively (Fig. 5A). Although amylase concentration in the sheet groups was high on day 1, the concentration sharply decreased to below 200 mU/ml on day 3.

Total amylase level was calculated by multiplying the amylase concentration and the abdominal fluid volume. The amylase level showed a similar tendency with amylase concentration (Fig. 5B). Control group showed a significantly higher level than the sheet groups on day1 and 3 ($p = 0.008$ at day 1 and 0.001 at day 3 in rADSC sheet, and $p = 0.024$ at day 1 and 0.019 at day 3 in rBMSC sheet). Amylase level showed greater difference with the amylase concentration between the control and the sheets group, because there was a significant reduction in the fluid collection from sheet groups as opposed to the control group. No significant difference in the amylase concentration and level was observed between the rADSC and rBMSC sheet groups.

3.6. Immunomodulatory effects of rADSC sheet and rBMSC sheet on pancreas resection site

In the rADSC sheet group, some red blood cells were wedged in, and the sheet attatchment was confirmed with the naked eye; such observations were not seen in the rBMSC sheet group (data not shown). Immune responses of rADSC and rBMSC sheets were examined with the immune array kit to confirm the possibility of inflammation and pancreatitis. On day 7 post operation, the area 3 mm towards the pancreatic head from the pancreatic resection surface was removed from normal rats, DP as a control, DP with rADSC sheet group, and DP with rBMSC sheet group. In the DP group, adhesion and immune markers, including soluble ICAM (CD54), LIX, L-selectin, Thymus chemokine, TIMP-1, showed increased levels compared to normal rats. The ADSC attachment group showed higher levels of soluble ICAM-1 (CD54), L-selectin, thymus chemokine, and TIMP-1 compared with other groups. The BMSC attachment group showed no expression or significantly lower levels of said proteins compared with control group and rADSC sheet group (Fig. 6).

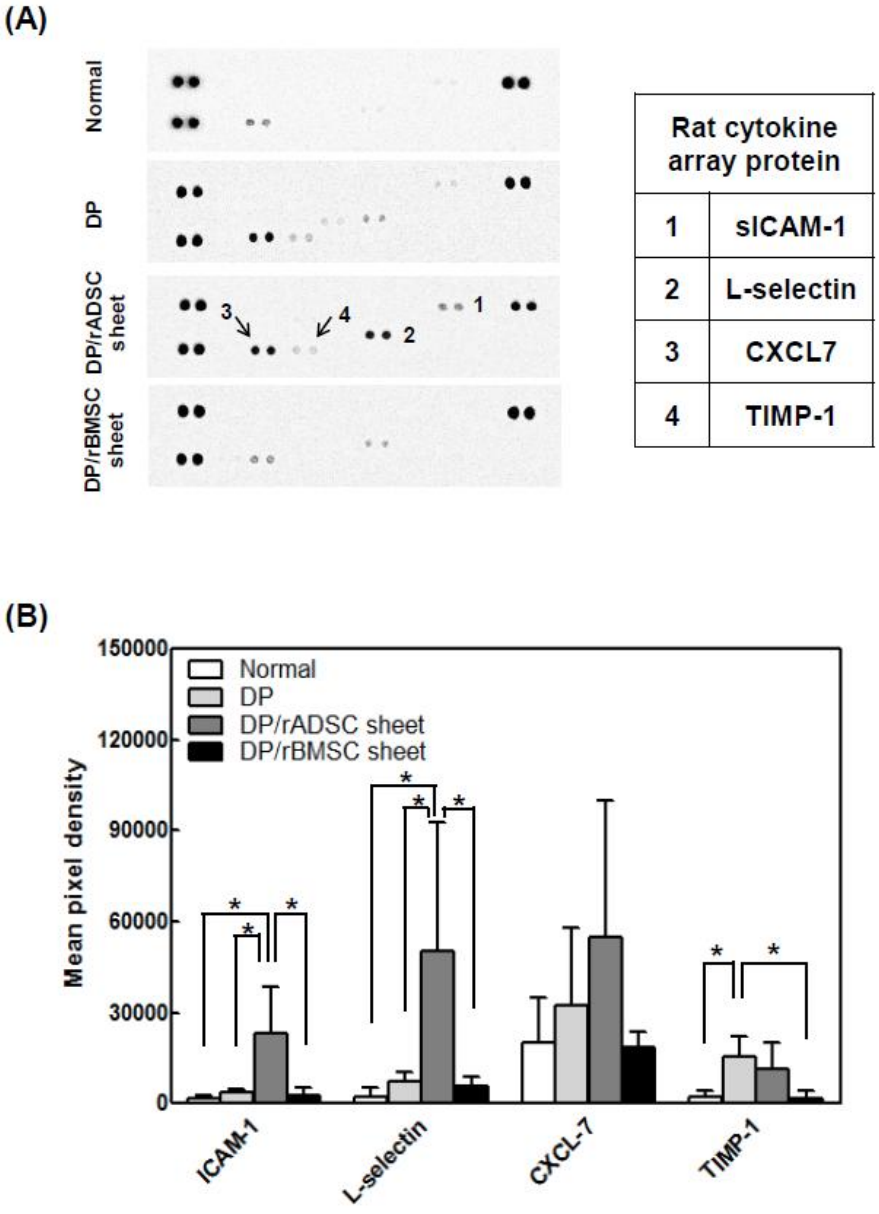

Fig. 6. Rat cytokine array for detection immunomodulatory effects of the rADSC sheet and rBMSC sheet on the pancreas resection site. The remaining pancreas of untreated rats (normal), DP as a control, rADSC sheet attached with DP, and a rBMSC sheet attached with DP on day 7 post-operation. (A) Representative membranes and (B) selective quantification are shown for the tissues of each group. Selective quantification markers include soluble ICAM (CD54), LIX, L-selectin, thymus chemokine, and TIMP-1.

3.7. Immunohistochemistry and H&E staining for cell sheet attachment

To confirm that the cell sheets remain attached to the resection surface for prolonged period, transplanted cells were detected by GFP fluorescence. Many tissues and blood cells have

autofluorescence; therefore, in order to remove autofluorescence and specifically identify the transplanted cells, IHC of anti-GFP was used instead of directly identifying the green fluorescence of GFP. DAB staining was performed with a GFP antibody. When the tissues were examined on 1 and 3 days post-operation, cell sheets adhering to the duct were observed (Fig. 7). H&E staining of the same sites was performed. Although all groups including DP, rADSC sheet with DP, and rBMSC sheet with DP showed inflammatory cells accumulation on the resection site, the transplanted sheets were firmly attached onto the resection sites and the presence of extracellular matrix barrier on day 1 was confirmed. On day 3, sheet groups showed decreased inflammatory response, and regeneration started to take place around the transplantation sites. Importantly, a dense layer of regenerated tissue and adhesion of other organs to the exposed surface of the transplanted rADSC sheet was observed.

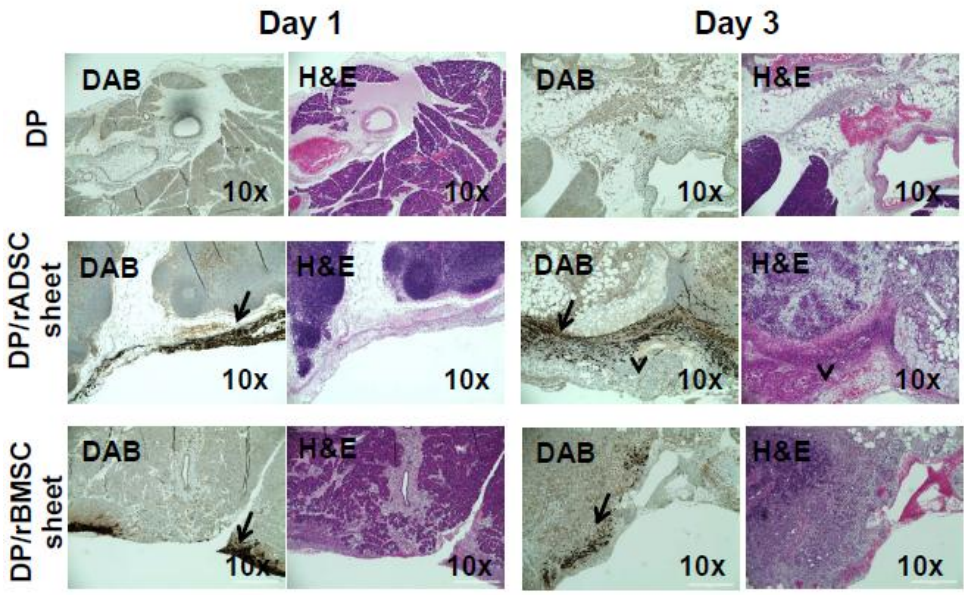

Fig. 7. Histological and immunohistochemical analysis of the pancreas of DP, rADSC sheet after DP, rBMSC sheet after DP on days 1 and 3. (A) Immunohistochemical staining for GFP rADSC and GFP rBMSC. Arrow indicates transplanted cells on the resection surface. Scale bars represent 400 μm. GFP cells that adhered to the ducts were observed in rADSC and rBMSC sheet groups on day 1 and 3. (B) H&E staining of the next slides of IHC tissues. While all groups showed inflammatory cell accumulation at the resection site on day 1, the sheet transplanted groups showed reduced inflammatory response and regeneration started to occur around the transplantation site on day 3. A dense layer of regenerated tissue and adhesion to other organs to the exposed surface of the transplanted rADSC sheet was observed (arrow ahead).

4. Discussion

While there has been significant improvement in pancreatic surgical techniques, pancreatic fistula still occurs at a high rate. POPF is a serious life-threatening complication that significantly prolongs hospital stay and increases healthcare costs.[16] Substantial effort has been made to prevent pancreatic fistula, such as modifying the surgical procedure and drainage regime, and selecting materials that can minimize the occurrence of POPF [3-5, 17, 18]; however, a definitive approach for preventing POPF is still lacking.[6, 7] Several studies have reported that fibrin glue sealant or polyglycolic acid felt can reduce the pancreatic anastomotic leak, but other reports have shown contrasting findings.[19-22] These controversial results indicate that the current materials in use are not sufficient to prevent pancreatic fistula. These materials are difficult to be applied onto wet and rough surfaces, and do not induce tissue regeneration but rather simply serve as a passive barrier for inflammation and fluid intake.[23] The characteristics of an ideal material for preventing POPF include flexibility, biocompatibility, adhesiveness, and ability to induce wound healing at the resection site. The physical and biological properties of materials should be considered prior to clinical application. Therefore, the application of mesenchymal stem cells (MSCs) for preventing POPF is a promising approach because MSCs have regeneration ability and immune modulation function. Recently, many clinical studies have reported the successful clinical application of MSCs for wound healing[24-26] and immune diseases.[27]

Despite the advantages of cell therapy using MSCs, traditional single cell injection method is difficult to be applied to local regions because of massive cell loss and low survival rate of cells. Hence, a novel technique for efficiently transplanting cells to target regions is needed. We hypothesized that mesenchymal stem cell sheets would effectively attach onto the pancreas resection site, and induce regeneration, wound healing, and immune modulation. Cell sheet technology is one of the most highly promising approaches of cell and tissue therapy in terms of clinical application. Cell sheets are harvested by controlling their

temperature, which enables them to maintain their shape; also, adhesion protein layers facilitate attachment to the tissue surface and cell-cell interaction, thereby acting like a small tissue [9, 10].

In this study, we first established a rat model of POPF that recapitulates actual clinical settings. When we performed distal pancreatectomy at the pancreatic tail near the spleen, the rat's pancreas adhered to other organs and did not reveal any signs of pancreatic fistula (model III). We therefore hypothesized that the duct has to be large enough to generate pancreatic fistula. We divided the parenchym in the direction of the pancreas head and ligated the same site duct to prevent bile leakage. As a result, plenty of fluid was generated and the presence of pancreatic fistula was confirmed amylase concentration measurement. However, in model I, the entire control group died one day after the surgery, and the cell sheet transplanted groups also died three days post operation. Thus, this model generated an excessively severe pancreatic fistula that made it unreliable to detect the effect of the materials designed to prevent POPF. We then injured the splenic and gastric duct (model II) at a position close to the portal vein and performed distal pancreatectomy and splenectomy, considering recent studies which have generated POPF models by cutting the splenic duct and We then injured the splenic and gastric duct (model II) at a position close to the portal vein and performed distal pancreatectomy and splenectomy; this approach is different from that of a recent study which generated POPF model by cutting the splenic duct and leaving the pancreas itself intact.[28, 29] As mentioned above, pancreatic fistula can be generated by cutting the splenic duct even with considering the rapid healing ability of rats, but the opening of the distal duct without parenchymal resection ultimately led to obstructive pancreatitis with leakage of pancreatic juice in the previous type I model, which confounded the experimental results. The result suggests potential problems not only in the rats' healing ability but also in the reliability of their modeling method. Furthermore, our modeling highly resembles the clinical approach, making it a more applicable method.

We fabricated mesenchymal stem cell sheets using rat adipose-derived stem cells (rADSC) and rat bone marrow stem cells (rBMSC) on temperature sensitive UpCell culture dishes. After lowering the temperature of the dish to 20 °C, we were able to procure firm cell sheets that could be easily handled with the CellShifter membrane. CellShifter™ membrane was employed to help the cell sheet retain its morphology with adhesion molecules and was then removed after transporting the cell sheet onto the transplantation surface. In this study, we isolated two different types of MSCs from the adipose tissue and the bone marrow. ADSC, which are often used in regenerative therapies, can be acquired repeatedly[30] and grow rapidly. They are multipotent cells, and secrete a wide range of regenerative factors. BMSC are also studied as another viable source of mesenchymal stem cells for cellular therapy. They are reported to have exceptional potential in differentiation and immune modulation abilities.[31-33]

POPF are assessed in clinics by measuring the amylase concentration and fluid of ascites. In fact, POPF is a concept that includes not only the leakage,of post-operative pancreatic juice but also various clinical consquences sometimes life threatening (intraperitoneal inflammation sometimes abscess formated with or without sepsis, deleyed gastric emptying, etc.). [34] However, considering the causal relationship, leakage of the pancreatic juice is the cause and leads to such clinical consquences. If the leakage of the pancreatic juice can be prevented, the incidence of complications such as intraperitoneal infection or delayed gastric emptying will naturally decrease, POPF and pancreatic juice leakage except the concept including clinical consequences were treated the same way in this study. In our experiment, there was a significant difference in the amount of fluid and amylase level between the control and sheet application groups. In the control group, the amount of ascites collected was approximately 3 ml after one week. In the sheet transplanted group, however, only 1.55 ml was collected in the rADSC group, and 0.55 ml was collected in the rBMSC group immediately after transplantation, and these amounts decreased rapidly over time and finally

were depleted after one week. A similar pattern was observed in MR images as well. To confirm the presence of pancreatic juice in the abdominal fluid collection, amylase concentration and level were each measured on days 1, 3 and 7. Amylase concentration and level showed a similar pattern with abdominal fluid volume. Both cell sheets demonstrated potential in inhibiting POPF. Abdominal fluid volume and amylase concentration between the two sheet groups did not show significant difference.

To confirm the attachment and survival of the transplanted cells, we isolated cells from GFP transgenic rats. The transplanted rADSC and BMSC were attached to the resection site in their intact sheet form. After three days, rADSC and rBMSC were not only attached but were proliferating on the surface. Interestingly, the rADSC transplanted group showed high degree of adherence to other organ and tissues in the abdomen. We suspect that these results are relevant to the studies that suggest ADSC recruit adhesion and regeneration factors such as FGF-2, VEGF, and HGF.[35] However, BMSC showed no visible adhesion within the abdomen. A similar tendency was demonstrated in the immune cytokine array as well. The results of immune cytokine array indicated a dramatic increase in soluble ICAM-1, a type of adhesion protein, only in the ADSC sheet transplanted group compared to the normal, control, and rBMSC sheet transplanted group. Also, the rADSC transplanted group showed the increase the level of other molecules related to wound healing and immune cytokines, such as L-selectin, CXCL7, and TIMP-1. Conversely, rBMSC sheet showed lessened immune reaction compared to control and rADSC sheet group. Although ADSCs are easy to acquire and fabricate into cell sheets for preventing pancreatic fistula, it is necessary to consider the inflammatory reaction to organ adhesion. On the other hand, BMSC have a remarkable advantage of regulating immune reaction and promoting regeneration.[36] These two types of cell sheets both prevent pancreatic fistula, but a better model that reconciles the challenges in each sheet is needed. We plan to apply our experimental design onto a larger porcine model to ensure a faithful adaptation to clinical results.

In our current study, we established a relevant animal model for POPF in rats to evaluate the current materials used for preventing POPF, which was constructed via splenic duct resection with distal pancreatectomy. Mesenchymal stem cell (MSC) sheets were fabricated on temperature sensitive dishes, and MSCs sheets significantly decreased abdominal fluid volume and amylase level compared to those of the control group. These measurements were confirmed with MR images. By tracking GFP expressing MSCs after transplantation, the cell sheets were found to be firmly attached on the resection surface on day 1, and were shown to have proliferated on day 3. While rADSC sheet induced adhesion to other tissues in the abdomen, rBMSC sheet did not show adhesion within the abdomen and rather lessened immune reaction at the pancreatic resection site. This new technology has the potential to be translated to clinical settings in all kinds of pancreatic surgery, especially, pancreatic enucleation and pancreatic wedge resection in order to fulfill the unmet need of POPF.

5. Conclusion

MSCs sheet technology is a promising approach to prevent POPF by effectively delivering the cells to the resection sites. Also, these MSCs induce regeneration and immune modulation at the resection site. However, more preclinical studies are needed to translate this novel technology to clinical practice.

References

[1] C. Bassi, C. Dervenis, G. Butturini, A. Fingerhut, C. Yeo, J. Izbicki, J. Neoptolemos, M. S arr, W. Traverso, M. Buchler, I.S.G.P. Fist, Postoperative pancreatic fistula: An international s tudy group (ISGPF) definition, Surgery 138(1) (2005) 8-13.

[2] P.M. Sell NM, Gabale S, Leiby BE, Rosato EL, Winter JM, Yeo CJ, Lavu H., The influen ce of transection site on the development of pancreatic fistula in patients undergoing distal pa ncreatectomy: A review of 294 consecutive cases., Surgery 157(6) (2015) 1080-7.

[3] H. Akita, et al., Closure method for thick pancreas stump after distal pancreatectomy: soft coagulation and polyglycolic acid felt with fibrin glue. , Langenbeck's Archives of Surgery, 400(7) (2015) 843-848.

[4] J.S. Park, et al., Use of TachoSil((R)) patches to prevent pancreatic leaks after distal panc reatectomy: a prospective, multicenter, randomized controlled study., Journal of Hepato-Bilia ry-Pancreatic Sciences 23(2) (2016) 110-117.

[5] M. Weniger, et al., Autologous but not Fibrin Sealant Patches for Stump Coverage Reduc e Clinically Relevant Pancreatic Fistula in Distal Pancreatectomy: A Systematic Review and Meta-analysis., World Journal of Surgery 40(11) (2016) 2771-2781.

[6] T. Hackert, M.W. Buchler, Randomized clinical trial of isolated Roux-en-Y versus conve ntional reconstruction after pancreaticoduodenectomy (Br J Surg 2014; 101: 1084-1091), Br J Surg 101(9) (2014) 1092.

[7] A. McKay, S. Mackenzie, F.R. Sutherland, O.F. Bathe, C. Doig, J. Dort, C.M. Vollmer, Jr., E. Dixon, Meta-analysis of pancreaticojejunostomy versus pancreaticogastrostomy reconstr uction after pancreaticoduodenectomy, The British journal of surgery 93(8) (2006) 929-36.

[8] Q.Y. Chen G, Niu L, DI T, Zhong J, Fang T, Yan W., Application of the cell sheet techniq ue in tissue engineering., Biomed rep 3(6) (2015) 749-757.

[9] Y.N. Okano T, Sakai H, Sakurai Y., A novel recovery system for cultured cells using plas ma-treated polystyrene dishes grafted with poly(N-isopropylacrylamide). J biomed Mater Re s 27(10) (1993) 1243-51.

[10] M.Y. Ai Kushida, Chie Konno, Akihiko Kikuchi, Yasuhisa Sakurai, Teruo Okano, Decre ase in culture temperature releases monolayer endothelial cell sheets together with deposited

fibronectin matrix from temperature-responsive culture surfaces, J biomed Mater Res 45 (19 99) 355-362.

[11] M.Y. Joseph Yanga, Kohji Nishidab, Takeshi Ohkic, Masato Kanzakid, Hidekazu Sekine a, Tatsuya Shimizua, Teruo Okanoa, Cell delivery in regenerative medicine: The cell sheet en gineering approach, J Control Release. 116(2) (2006) 193-203.

[12] Y.M. Kanai N, Okano T., Cell sheets engineering for esophageal regenerative medicine., Ann Transl Med 2(3) (2014) 193-203.

[13] T. Ohki, et al., Prevention of esophageal stricture after endoscopic submucosal dissectio n using tissue-engineered cell sheets., Gastroenterology 143(3) (2012) 582-8 e1-2.

[14] S.G. Ruchi Rastogi, Bhavya Garg, Sandeep Vohra, Manav Wadhawan, Harsh Rastogi, C omparative accuracy of CT, dual-echo MRI and MR spectroscopy for preoperative liver fat q uantification in living related liver donors, Indian journal of radiology and imaging 26(1) (20 16) 5-14.

[15] G.H. Mark Bydder, Takeshi Yokoo, Claude B. Sirlin Optimal phased-array combination for spectroscopy., Magnetic Resonance Imaging 26(6) (2008) 847-850.

[16] D. Dindo, N. Demartines, P.A. Clavien, Classification of surgical complications: a new proposal with evaluation in a cohort of 6336 patients and results of a survey, Ann Surg 240 (2) (2004) 205-13.

[17] W.E. Fisher, C. Chai, S.E. Hodges, M.F. Wu, S.G. Hilsenbeck, F.C. Brunicardi, Effect of BioGlue on the incidence of pancreatic fistula following pancreas resection, J Gastrointest S urg 12(5) (2008) 882-90.

[18] G. Farkas, L. Leindler, G. Farkas, Jr., Safe closure technique for distal pancreatic resecti on, Langenbecks Arch Surg 390(1) (2005) 29-31.

[19] Y. Suzuki, Y. Kuroda, A. Morita, Y. Fujino, Y. Tanioka, T. Kawamura, Y. Saitoh, Fibrin g lue sealing for the prevention of pancreatic fistulas following distal pancreatectomy, Arch Su rg 130(9) (1995) 952-5.

[20] H.B. Kram, S.R. Clark, H.P. Ocampo, M.A. Yamaguchi, W.C. Shoemaker, Fibrin glue s ealing of pancreatic injuries, resections, and anastomoses, Am J Surg 161(4) (1991) 479-81; discussion 482.

[21] A.A. D'Andrea, V. Costantino, C. Sperti, S. Pedrazzoli, Human fibrin sealant in pancreat

ic surgery: it is useful in preventing fistulas? A prospective randomized study, Ital J Gastroen terol 26(6) (1994) 283-6.

[22] B. Suc, S. Msika, A. Fingerhut, G. Fourtanier, J.M. Hay, F. Holmieres, B. Sastre, P.L. Fa gniez, R. French Associations for Surgical, Temporary fibrin glue occlusion of the main panc reatic duct in the prevention of intra-abdominal complications after pancreatic resection: pros pective randomized trial, Ann Surg 237(1) (2003) 57-65.

[23] B. Suc, S. Msika, A. Fingerhut, G. Fourtanier, J.M. Hay, F. Holmieres, B. Sastre, P.L. Fa gniez, Temporary fibrin glue occlusion of the main pancreatic duct in the prevention of intra-abdominal complications after pancreatic resection: prospective randomized trial, Ann Surg 237(1) (2003) 57-65.

[24] Y. Wu, L. Chen, P.G. Scott, E.E. Tredget, Mesenchymal stem cells enhance wound heali ng through differentiation and angiogenesis, Stem Cells 25(10) (2007) 2648-59.

[25] S.W. Kim, H.Z. Zhang, L. Guo, J.M. Kim, M.H. Kim, Amniotic mesenchymal stem cell s enhance wound healing in diabetic NOD/SCID mice through high angiogenic and engraftm ent capabilities, Plos One 7(7) (2012) e41105.

[26] L. Shin, D.A. Peterson, Human mesenchymal stem cell grafts enhance normal and impa ired wound healing by recruiting existing endogenous tissue stem/progenitor cells, Stem Cell s Transl Med 2(1) (2013) 33-42.

[27] M.d.P. Martínez-Montiel, G.J. Gómez-Gómez, A.I. Flores, Therapy with stem cells in in flammatory bowel disease, World Journal of Gastroenterology : WJG 20(5) (2014) 1211-122 7.

[28] T. Tanaka, et al., Development of a novel rat model with pancreatic fistula and the preve ntion of this complication using tissue-engineered myoblast sheets., Journal of Gastroenterol ogy 48(9) (2013) 1081-1089.

[29] H. Kaneko, et al., Novel therapy for pancreatic fistula using adipose-derived stem cell s heets treated with mannose. , Surgery (2017).

[30] P.E.D. Laura Frese, and Simon P. Hoerstrup, Adipose Tissue-Derived Stem Cells in Reg enerative Medicine, Transfus Med hemother 43(4) (2016) 268-274.

[31] R.F. Brazelton TR, Keshet GI, Blau HM, From marrow to brain: expression of neuronal phenotypes in adult mice., Science 290 (2000) 1775-1779.

[32] M.W. Grant MB, Caballero S, Brown GA, Guthrie SM, Mames RN, Byrne BJ, Vaught T, Spoerri PE, Peck AB, Scott EW., Adult hematopoietic stem cells provide functional hemangi oblast activity during retinal neovascularization., Nat med 8 (2002) 607-612.

[33] B.A. Bunnell, A.M. Betancourt, D.E. Sullivan, New concepts on the immune modulatio n mediated by mesenchymal stem cells, Stem Cell Research & Therapy 1(5) (2010) 34.

[34] S. Hajibandeh, S. Hajibandeh, R.M.A. Khan, S. Malik, M. Mansour, A. Kausar, D. Suba r, Stapled anastomosis versus hand-sewn anastomosis of gastro/duodenojejunostomy in panc reaticoduodenectomy: A systematic review and meta-analysis, International Journal of Surge ry (2017).

[35] E.J.C. Naghmeh Naderi, Michelle Griffin,Tina Sedaghati,Muhammad Javed,Michael W Findlay,Christopher G Wallace,Afshin Mosahebi,Peter EM Butler,Alexander M Seifalian, Iai n S Whitaker, The regenerative role of adipose-derived stem cells (ADSC) in plastic and reco nstructive surgery, international wound journal 14 (2016) 112-124.

[36] A.M.B. Bruce A Bunnell, and Deborah E Sullivan, New concepts on the immune modul ation mediated by mesenchymal stem cells, Stem cell res ther 1(5) (2010) 34.

국문요약

췌장 절제 이후에 발생하는 췌장루는 매우 치명적인 수술 후 합병증이다. 이 췌장루의 발생을 최소화 하기 위하여 많은 실질적인 노력들이 거듭되어 왔으나 아직까지도 확실한 방지법은 없는 상태이다. 우리는 실험을 통해 측정 가능한 췌장루를 쥐모델에서 만들 수 있었다. 실험에 사용 된 쥐의 지방유래 줄기세포와 골수유래 줄기세포는 간엽줄기세포의 특성뿐만 아니라 손상되지 않은 피브로넥틴으로 세포와 세포 접합부와 접합 단백질을 유지했다. 수술 후 1, 3, 7 일에 자기공명영상 이미지와 복강내 저류액에서 관찰 된 바와 같이, 쥐의 지방유래 줄기세포 시트와 골수유래 줄기세포 시트를 이식 받은 쥐 들에서 대조군에 비해 복강내 저류액의 양이 현저하게 감소됨을 관찰 할 수 있었다. 아밀라아제 농도와 총 아밀라아제 함량은 대조군과 비교하여 쥐의 지방유래 줄기세포 시트 이식군과 골수유래 줄기세포 시트 이식군에서 유의하게 낮았다. 쥐의 지방유래 줄기세포 시트는 증가된 접합 및 면역 사이토카인 프로파일을 보인 반면, 쥐의 골수유래 줄기세포 시트는 대조군 및 쥐의 지방유래 줄기세포 시트에 비하여 감소된 면역반응을 보였다. 우리의 결과는 간엽줄기세포 시트 기술이 췌장루를 방지하는 데 사용될 수 있다는 것을 보여주며, 이 새로운 기술은 현재의 췌장루 방지 기술의 부족한 면을 보완하기 위해 임상에 적용될 수 있는 충분한 잠재력이 있다.